# Ultrafast Energy Transfer from Chlorophyll c2 to Chlorophyll a in Fucoxanthin–Chlorophyll Protein Complex

**ARTICLE** *in* JOURNAL OF PHYSICAL CHEMISTRY LETTERS · NOVEMBER 2013

Impact Factor: 7.46 · DOI: 10.1021/jz401919k

THE JOURNAL OF PHYSICAL CHEMISTRY Letters

Letter

pubs.acs.org/JPCL

# Ultrafast Energy Transfer from Chlorophyll $c_2$ to Chlorophyll *a* in Fucoxanthin–Chlorophyll Protein Complex

Egidijus Songaila,[†] Ramūnas Augulis,[†] Andrius Gelzinis,[†,‡] Vytautas Butkus,[†,‡] Andrew Gall,[§] Claudia Büchel,[∥] Bruno Robert,[§] Donatas Zigmantas,[⊥] Darius Abramavicius,[‡,#] and Leonas Valkunas*[,†,‡]

[†]Center for Physical Sciences and Technology, Savanoriu Avenue 231, 02300 Vilnius, Lithuania

[‡]Department of Theoretical Physics, Faculty of Physics, Vilnius University, Sauletekio 9-III, 10222 Vilnius, Lithuania

[§]CEA, Institute of Biology and Technology of Saclay, UMR 8221 CNRS, 91191 Gif sur Yvette, France

[∥]Institut für Molekulare Biowissenschaften, Universität Frankfurt, Max-von-Laue-Straße 9, Frankfurt, Germany

[⊥]Department of Chemical Physics, Lund University, P.O. Box 124, 22100 Lund, Sweden

[#]State Key Laboratory of Supramolecular Complexes, Jilin University, 2699 Qianjin Street, Changchun 130012, People's Republic of China

**ABSTRACT:** Light-harvesting in fucoxanthin-chlorophyll protein (FCP) of diatoms is performed by a cluster of chromophores: chlorophylls *a* (Chl *a*), chlorophylls $c_2$ (Chl $c_2$), and carotenoids fucoxanthins. It is well-known that energy captured by fucoxanthin is transferred to Chl *a* on a subpicosecond time scale. However, the energy flow channel connecting Chl $c_2$ and Chl *a* remained elusive. In this study, the energy transfer between Chl $c_2$ and Chl *a* molecules in the FCP complex from the diatom algae *C. meneghiniana* at room temperature is investigated using pump–probe and coherent two-dimensional electronic spectroscopy. Measured dynamics of the absorption band associated with the $Q_y$ transition of the Chl $c_2$ reveals an ultrafast energy transfer pathway to Chl *a*. This conclusion is supported by the theoretical simulations based on the effective oscillator model.

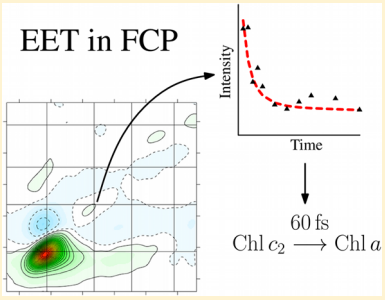


**SECTION:** Energy Conversion and Storage; Energy and Charge Transport

The efficient light-harvesting antennae allow photosynthetic organisms to survive in different environments at various light intensities and wavelengths. This function of light-harvesting is realized by the constituent pigment molecules (chlorophylls, phycobilins, and carotenoids) arranged in various aggregated formations.[1] Diatoms are unicellular chromophyte algae inhabiting the ocean down to depths where the sunlight still penetrates. They are thought to be the most important group of eukaryotic phytoplankton accounting for nearly a quarter of the global primary production.[2] Like in the higher plants, light-harvesting function in diatoms is performed by intrinsic membrane proteins. The light-harvesting complex (LHC) of diatoms is usually named the fucoxanthin-chlorophyll protein (FCP), since it contains carotenoid fucoxanthin instead of xanthophylls present in the higher plants. Fucoxanthin absorbs light in the green-blue region, where light propagates the longest distances in water, thus allowing diatoms to harvest sunlight in underwater conditions.

The information on the molecular structure of FCP is very limited. Usually, structural arrangement of FCP is compared to the light-harvesting complex of Photosystem II (LHCII) from plants due to the high sequence homology.[3] However, in addition to the differences in pigment composition in both complexes (xanthophylls, chlorophylls *a* and *b* in LHCII vs fucoxanthin and chlorophylls *a* and $c_2$ in FCP), the pigment ratio is also different. LHCII complex contains 14 chlorophylls and 4 carotenoids,[4] while FCP contains more carotenoids per chlorophyll. Even though the exact number of pigments in the FCP complex is still debated, the ratio 4:4:1 of fucoxanthin, chlorophyll (Chl) *a* and Chl $c_2$ is well established.[5,6] The presence of Chl $c_2$ helps to increase the light absorption at longer wavelengths when compared to Chl *a* (especially in the Soret band). The FCP absorption spectrum in the $Q_y$ and $Q_x$ regions is shown in Figure 1.

Previous spectroscopic studies have established that the energy is efficiently transferred from fucoxanthin to Chl *a*.[5,8] Moreover, fast energy transfer from Chl $c_2$ to Chl *a* (on a time scale of <100 fs) was also anticipated, but remained unconfirmed. Thus, the role of Chl $c_2$ in energy transfer pathways in FCP is still under question.[9] In this paper, we present the results of the studies aimed at determination of the role of Chl $c_2$ in the FCP complex.

To investigate the interaction strength and excitation energy transfer efficiency between Chl $c_2$ and Chl *a* in the FCP complex at room temperature, pump–probe measurements were performed by pumping at different wavelengths. We expected the maximum absorption of Chl $c_2$ $Q_y$ band to occur at approximately 635 nm, so we paid special attention to that

**Received:** September 6, 2013
**Accepted:** October 9, 2013

   dx.doi.org/10.1021/jz401919k | *J. Phys. Chem. Lett.* 2013, 4, 3590–3595

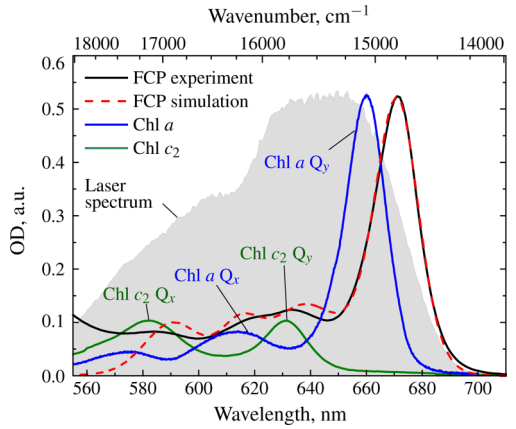


**Figure 1.** Absorption spectra of the FCP complex at 300 K: experimental (black solid line) and simulated (red dashed line); spectra of isolated Chl *a* in diethyl ether (blue solid line),[7] Chl $c_2$ in acetone (green solid line). Spectrum of the laser pulses used in the 2D ES experiments is represented by the gray shaded area.

excitation wavelength region. The pump−probe results are shown in Figure 2. Presented 2D plots are created by stacking sets of pump−probe spectra measured using various pump wavelengths. It can be clearly seen that at $t_{delay}$ = 0 fs the spectrum is dominated by the ground state bleach and stimulated emission at approximately $\lambda_{pump}$ = 680 nm and $\lambda_{probe}$ = 680 nm and excited state absorption at shorter probe wavelengths. Both features can be attributed to the Chl *a* $Q_y$ band. In addition, this band is inhomogeneously broadened, which is indicated by diagonal elongation of the peaks. At later times, $t_{delay}$ = 200 fs and $t_{delay}$ = 1 ps, the bleach signal gradually becomes independent of the pump wavelength, indicating that most of the excitation reaches Chl *a*. Significant bleaching/stimulated emission around $\lambda_{pump}$ = 630−640 nm, $\lambda_{probe}$ = 680 nm indicates the energy transfer from Chl $c_2$ to Chl *a*. The dynamics of the excited state absorption contribution is difficult to interpret unambiguously. It is very likely that local heating contributes to it as well. Although pump−probe experiments give a clue that excitation is transferred from Chl $c_2$ to Chl *a* on a time scale of tens to hundreds of femtoseconds, the results are inconclusive due to several drawbacks of the pump−probe technique: limited simultaneous spectral and temporal resolution and temporal and amplitude jitter within a set of separately measured pump−probe spectra which are combined into a single 2D map.

To further investigate the Chl $c_2$→Chl *a* energy transfer, we performed coherent two-dimensional (2D) electronic spectroscopy (ES). This method is able to provide valuable information about the initial evolution of the excitation and allows to follow the details of the energy and charge transfer dynamics, exciton diffusion, as well as the environment relaxation.[10−15] It utilizes multiple pulse excitation with controlled delays between the pulses and measures amplitude and phase of the emitted signal. The temporal and spectral resolutions obtained in these experiments are not related.[16] 2D ES is free from the shortcomings of the pump−probe technique mentioned above.

In the experimental 2D spectra at the initial population time $t_2$ = 20 fs (see Figure 3), the Chl *a* $Q_y$ band at 14900 cm$^{-1}$ (670 nm) shows up as a dominating feature (note that we do not present spectra at earlier population times due to the presence of the pulse overlap effects). Another diagonal peak at 15600 cm$^{-1}$ (640 nm) related to the transition into the $Q_y$ band of Chl $c_2$ is rather weak, but also visible. The corresponding cross-peak below the diagonal can be identified as an elongation of the main diagonal peak along the $\omega_1$ axis. This indicates that Chl *a* and Chl $c_2$ are coherently coupled. The $Q_x$ band of Chl *a* at ∼16300 cm$^{-1}$ cannot be resolved on the diagonal; however, the lower cross-peak at $\omega_1$ = 16300 cm$^{-1}$ and $\omega_3$ = 14900 cm$^{-1}$ and upper crosspeak at $\omega_1$ = 14900 cm$^{-1}$ and $\omega_3$ = 16300 cm$^{-1}$ are visible. Diagonal peak caused by the Chl $c_2$ $Q_x$ absorption band at 16700 cm$^{-1}$ (598 nm) can hardly be distinguished, however, the corresponding cross-peak at $\omega_1$ = 16700 cm$^{-1}$ and $\omega_3$ = 14900 cm$^{-1}$ emerges at longer population times. Negative off-diagonal features at initial population times are attributed to the excited state absorption. A negative signal region is located directly above the diagonal peak that corresponds to the $Q_y$ transition of Chl *a*, but below the line at $\omega_3$ = 15600 cm$^{-1}$. This might be due to excited state absorption of a single Chl *a* molecule[17] or an indication that Chls *a* in the FCP complex form an excitonically coupled aggregate.[18,19]

Now we turn to time evolution of the 2D spectrum. The shape of the strongest diagonal peak becomes more round with increasing population time, while the nodal line between the positive and negative regions rotates. All these observations indicate the disappearance of correlation of exciton energy fluctuations, i.e., the system gradually loses its excitation frequency memory. Our data also shows the decay of the Chl *a* diagonal peak. If only the dynamics evolving during the initial 500 fs are considered, this decay can be well fitted with an exponential function with a time constant of ∼110 fs. Most

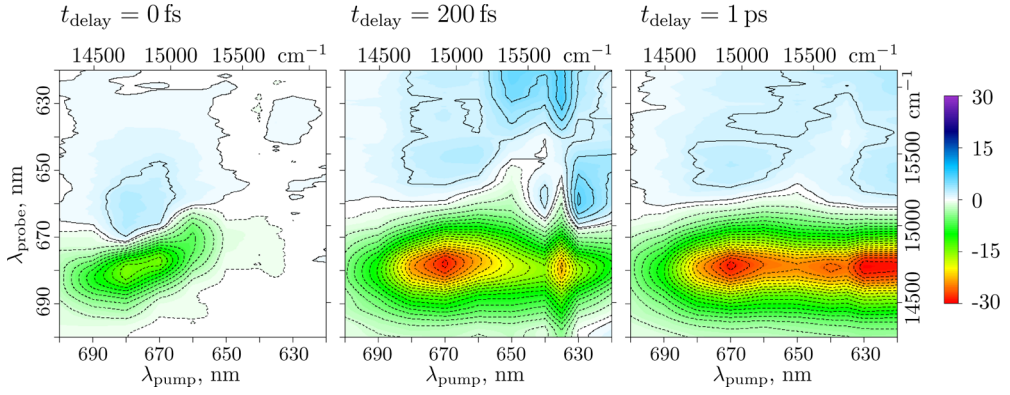


**Figure 2.** 2D maps of pump−probe data at three different population times. The plots are created by stacking sets of pump−probe spectra measured using various pump wavelengths. The *z* axis corresponds to ΔmOD.


dx.doi.org/10.1021/jz401919k | J. Phys. Chem. Lett. 2013, 4, 3590−3595

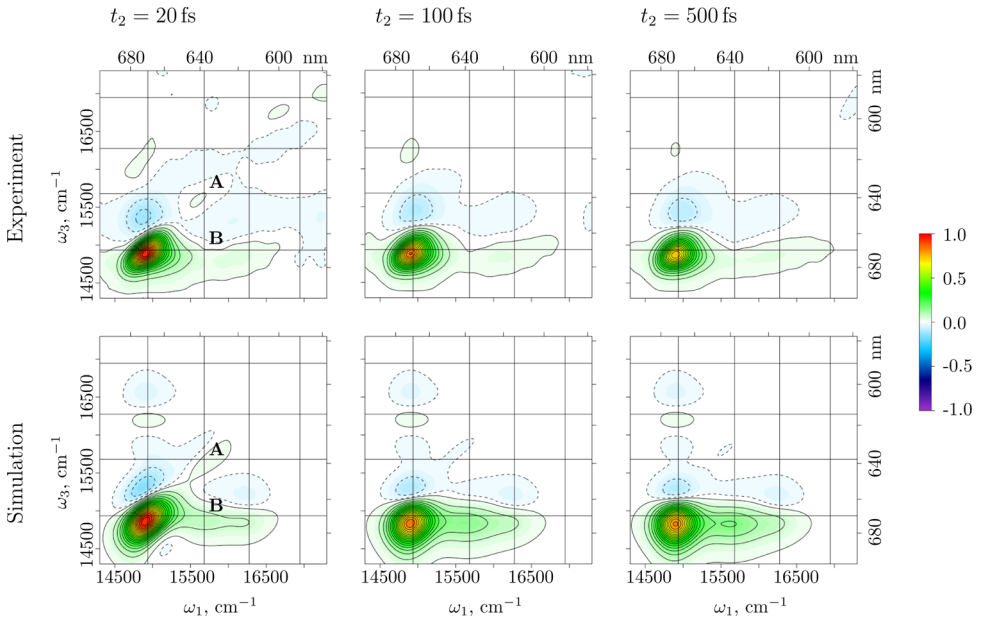


**Figure 3.** Experimental and simulated 2D spectra of the FCP complex at 300 K. Real (absorptive) part of the total (rephasing+nonrephasing) spectra is given. The spectra are scaled to the values of their respective maxima at $t_2$ = 20 fs. Horizontal and vertical lines correspond to the energies of single excitation bands (in order of decreasing energy: Chl *a* $Q_y$, Chl $c_2$ $Q_y$, Chl *a* $Q_x$, Chl $c_2$ $Q_x$) determined from the fitting procedure. Crossings of these lines denoted by **A** and **B** mark the Chl $c_2$ $Q_y$ diagonal peak and Chl $c_2$ $Q_y$–Chl *a* $Q_y$ cross-peak.

of the amplitude of this decay cannot be attributed to sample photodegradation, since in our experimental conditions the absorption spectrum changed by no more than 5% and peak amplitude decays by ∼30%. Some of this decay might be attributed to the initial line shape dynamics related to vibrational relaxation. In previous pump–probe measurements, the decay of the corresponding peak was shown to be multiexponential,[5] however, the fastest process detected was on the picosecond time scale due to the limited temporal resolution. Thus, our measurements show a very fast dynamics occurring in the Chl *a* region. This could be related to interactions of excited states of Chl *a* with a dark state (e.g., carotenoid $S_1$ state or a charge-transfer state), which would induce the decay of the Chl *a* population.[20,21]

The main aim of this study is unraveling energy transfer between the $Q_y$ states of Chl $c_2$ and Chl *a*. Hence, we focus onto the diagonal element of Chl $c_2$ and the corresponding cross-peak. The diagonal peak shows a clear exponential decay with the time scale of 60 fs (Figure 4a). Since Chl $c_2$ and Chl *a* are excitonically coupled, we interpret this as a signature of energy transfer. Surprisingly, no fast rising component is visible in the cross-peak evolution (Figure 4b). This could be explained if population from Chl *a* $Q_y$ is transferred downward on comparable time scale, as indicated by the decay of its diagonal peak. Then crosspeak dynamics would reflect two competing processes: transfer from Chl $c_2$ $Q_y$ to Chl *a* $Q_y$ and from this state to a lower energy dark state. Next we present simulations of the 2D spectra that support the conclusion that evolution of the 2D spectra indicates the ultrafast energy transfer from Chl $c_2$ to Chl *a* on the time scale of 60 fs.

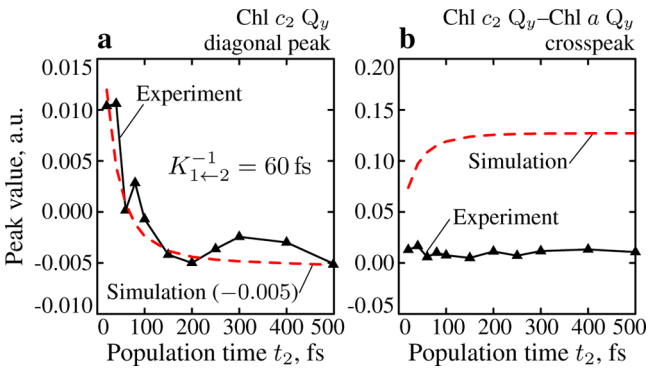


**Figure 4.** Time evolution of the Chl $c_2$ $Q_y$ diagonal peak (a) and Chl $c_2$ $Q_y$–Chl *a* $Q_y$ cross-peak (b).

As mentioned above, the structure of the FCP complex is not well-known. Explicit microscopic exciton model requires the knowledge about the spatial arrangement of the constituent molecules which is not available in this case. Therefore, we have developed an effective model of the FCP complex (similar to a four state model in ref 22) in order to simulate the 2D spectra. Our model and its relevant parameters are described below.

In the absorption spectra of the FCP complex (Figure 1), we can distinguish four bands corresponding to the $Q_y$ and $Q_x$ transitions of Chl *a* and Chl $c_2$. Each band is modeled as an anharmonic oscillator. The system Hamiltonian then is

$$\hat{H}_S = \sum_{e=1}^{4} \varepsilon_e \hat{A}_e^{\dagger} \hat{A}_e + \frac{1}{2} \sum_{e,e'=1}^{4} \Delta_{ee'} \hat{A}_e^{\dagger} \hat{A}_{e'}^{\dagger} \hat{A}_{e'} \hat{A}_e \qquad (1)$$

where $\varepsilon_e$ is energy of the $e$th band (exciton); $\Delta_{ee'}$ is the anharmonicity matrix, representing the binding energies of the excitons, and $\hat{A}_e^{\dagger}$ and $\hat{A}_e$ are the bosonic creation and annihilation operators of the $e$th exciton. As a result, we have 4 single exciton states and 10 double exciton states (4 overtone and 6 combination states).

We assume that all the environmental degrees of freedom constitute the heat bath, which consists of an infinite set of harmonic oscillators linearly coupled to the exciton subsystem. The bath-induced energy fluctuations of the exciton states are described using the bath spectral density. It is assumed that the energy fluctuations of different excitonic oscillators are


dx.doi.org/10.1021/jz401919k | J. Phys. Chem. Lett. 2013, 4, 3590–3595

uncorrelated. Here we use a composite spectral density represented by two Debye-type terms[23] describing fast and slow bath modes, respectively:

$$C_e''(\omega) = \frac{2\lambda_e^{\mathrm{F}}\gamma_{\mathrm{F}}\omega}{\omega^2 + \gamma_{\mathrm{F}}^2} + \frac{2\lambda_e^{\mathrm{S}}\gamma_{\mathrm{S}}\omega}{\omega^2 + \gamma_{\mathrm{S}}^2} \quad (2)$$

Reorganization energy $\lambda_e^{\mathrm{F(S)}}$ describes the coupling strength of the $e$th exciton band with the fast (slow) bath modes, and $\gamma_{\mathrm{F(S)}}^{-1}$ is the time scale of bath correlations. The fast bath modes are responsible for Lorentzian spectral profiles (homogeneous broadening), and the slow bath modes determine Gaussian spectral profiles (inhomogeneous broadening). We choose $\gamma_{\mathrm{F}}^{-1}$ = 50 fs and $\gamma_{\mathrm{S}}^{-1}$ = 10 ps, which are typical for biological pigment−protein complexes.[24]

The system is coupled to the classical electromagnetic field $\mathcal{E}$ by the dipolar system-field interaction Hamiltonian:

$$\hat{H}_{\mathrm{SF}} = -\sum_{e=1}^{4}\left(\mu_e\hat{A}_e^{\dagger} + \frac{1}{\sqrt{2}}\mu_e^{(2)}\hat{A}_e^{\dagger^2}\hat{A}_e + \mathrm{H.c.}\right)\cdot\mathcal{E} \quad (3)$$

Here $\mu_e$ is the vector determining the transition dipole moment from the electronic ground state to the $e$th exciton state, and $\mu_e^{(2)}$ is its anharmonic correction corresponding to the transitions from the single exciton state to the overtone state. For simplicity, we assume that all the dipoles are parallel and that the electric field pulses are $\delta$-shaped. These assumptions are perfectly justified as we consider an all−parallel 2D experiment with broadband pulses.

With this model, both linear and 2D spectra are calculated using the response function formalism employing the second-order cumulant expansion of the exciton energy correlations.[25,26] We used expressions given in ref 22. Free parameters to describe the experimental data then are: exciton energies $\varepsilon_e$, the anharmonicity matrix $\Delta_{ee'}$, reorganization energies $\lambda_e^{\mathrm{F(S)}}$, transition dipole moments $\mu_e$, and their corrections $\mu_e^{(2)}$. These parameters were obtained by numerical fitting.

From the linear absorption spectrum we can determine all the parameters relevant to the single exciton manifold. We used the Markov Chain Monte Carlo fitting procedure[27] and optimized exciton band energies $\varepsilon_e$, their transition dipole moments $\mu_e$ (peak intensities), and couplings with the bath $\lambda_e^{\mathrm{F(S)}}$ (homogeneous and inhomogeneous broadenings). The fitted model parameters are given in Table 1, whereas the simulated absorption spectrum is shown in Figure 1 by the red dashed line.

To simulate the 2D spectra, we also need to describe the parameters of the double exciton states. Their energies are $\varepsilon_e + \varepsilon_{e'} + \Delta_{ee'}$. Transitions to the combination exciton states are fully described by $\mu_e$, while transitions to the overtone states are described by $\mu_{e,ee} = \sqrt{2}\,\mu_e + \mu_e^{(2)}$. From the fit of cuts of the 2D spectra at $\omega_1 = \varepsilon_e$ along the $\omega_3$ axis, we obtained values of $\Delta_{ee'}$ and $\mu_e^{(2)}$. Transition dipole corrections are provided in Table 1, while the nonzero anharmonicity matrix values are $\Delta_{11}$ = 510 cm$^{-1}$, $\Delta_{21}$ = 150 cm$^{-1}$, $\Delta_{22}$ = 270 cm$^{-1}$, $\Delta_{31}$ = 235 cm$^{-1}$, and $\Delta_{32}$ = 150 cm$^{-1}$.

Energy transport between the exciton states is described by the transfer rates $K_{e'\leftarrow e}$. Since the diagonal peak of exciton $e$ = 2 (Chl $c_2$ $Q_y$ band) exhibits clear exponential decay, we set $K_{1\leftarrow 2}^{-1}$ = 60 fs. The corresponding upward excitation transport rate $K_{2\leftarrow 1}^{-1}$ = 2000 fs is calculated from the detailed balance relation.[25] Apart from energy transfer between the pigments, there could be other processes in FCP. Internal conversion in Chl $a$ would manifest as decay of the Chl $a$ $Q_x$ diagonal peak and the rise of the corresponding crosspeak. We do not resolve these signatures in our experimental spectra. Therefore no other transport rates were used in the simulations.

Our simulated 2D spectra are in good agreement with the experimental results (Figure 3). The shape of the main diagonal peak at initial population time $t_2$ = 20 fs as well as its qualitative evolution are well reproduced. The excited state absorption feature above the diagonal peak is recovered by including large anharmonic shift of the $Q_y$ overtone state of Chl $a$. The rotation of the nodal line in the intersection of positive and negative regions is also reproduced. Simulated spectra match the diagonal peak corresponding to the $Q_y$ transition of Chl $c_2$ and elongated peak below the diagonal.

Here we discuss the evolution of the peaks related to the $Q_y$ band of Chl $c_2$. Simulated temporal evolutions of the corresponding diagonal and off-diagonal peaks are presented in Figure 4. Even though the simulated curve for the cross-peak does not match the experimental dynamics, the diagonal peak dynamics fit the experiment almost perfectly. Simulations thus indicate that experimentally observed diagonal peak kinetics can be readily explained by the $K_{1\leftarrow 2}^{-1}$ = 60 fs excitation energy transfer rate. Adding a dark state to the model should help to reduce the deviations from experimental dynamics of the crosspeak, but the relevant parameters of this state are completely undetermined. We thus find that theoretical modeling supports the ultrafast energy transfer from Chl $c_2$ to Chl $a$.

Our results agree with a previous study,[5] which suggested an ultrafast energy transfer from Chl $c_2$ to Chl $a$ in FCP complex. It should be due to excitonic coupling between the pigments, which manifests itself as a crosspeak in 2D data. Note that while no signatures of excitonic coupling between Chl $a$ and Chl $c_2$ could be resolved in circular dichroism spectra,[28] it might be related to weak transition dipole moment of Chl $c_2$ $Q_y$ transition or spatial configuration of the molecules resulting in no rotational strength. Energy transfer from Chl $c_2$ to Chl $a$ was also studied in peridinin−chlorophyll protein (PCP) LHC from *Amphidinium carterae*,[29] which is similar in pigment stoichiometry to FCP complex. Global analysis of transient absorption spectra recorded after excitation of Chl $c_2$ $Q_y$ band gave time components of 75 fs and 1.4 ps. It was proposed that the longer component corresponds to the energy transfer between Chl $c_2$ and Chl $a$, although some fraction of energy is transferred on the shorter time scale. Our results show that in FCP complex excitation is transferred from Chl $c_2$ to Chl $a$ on 60 fs time scale, similar to 75 fs time scale in the PCP.[29] While we see some indications that a longer component exists, we can

**Table 1. Single Exciton Band Parameters Determined by Fitting the Linear Absorption Spectrum and Transition Dipole Corrections Obtained from the Fit of the 2D Spectra**

| | single exciton band[a] | | | |
|---|---|---|---|---|
| parameter | 1 | 2 | 3 | 4 |
| $\varepsilon_e$ [cm$^{-1}$] | 14935 | 15680 | 16275 | 16945 |
| $\mu_e$ ($x$) [a. u.] | 1 | 0.57 | 0.38 | 0.45 |
| $\lambda_e^{\mathrm{F}}$ [cm$^{-1}$] | 100 | 55 | 60 | 115 |
| $\lambda_e^{\mathrm{S}}$ [cm$^{-1}$] | 5 | 155 | 50 | 105 |
| $\mu_e^{(2)}(x)$ [a.u.] | −0.72 | −0.13 | 0 | 0 |

[a]We enumerate the single exciton bands $e$ = {1,2,3,4} corresponding to the Chl $a$ $Q_y$, Chl $c_2$ $Q_y$, Chl $a$ $Q_x$ and Chl $c_2$ $Q_x$ transitions, respectively.


dx.doi.org/10.1021/jz401919k | J. Phys. Chem. Lett. 2013, 4, 3590−3595

not resolve its time scale. However, to be consistent with our data, it must have considerably smaller amplitude than the shorter component, as opposed to ref 29.

Earlier, the Chl *a* absorption band at ∼620 nm was assigned to vibrational progression of $Q_y$ band and $Q_x$ band was placed at shorter wavelengths.[30] Here, we follow the recent results from ref 31, where it was shown that ∼620 nm band contains significant contributions from $Q_x$ transition. Our experimental 2D spectra do not show any clear vibrational signatures (though this might be related to the experimental time resolution). Thus we do not consider vibrational influence in our model.

In summary, we have performed both pump−probe and 2D ES experiments addressing the question of energy transfer in the FCP complex. Although the pump−probe results were inconclusive, 2D data showed that energy is transferred from Chl $c_2$ to Chl *a* on a 60 fs time scale. To verify the assignment of the ultrafast energy transfer, we performed simulations of the 2D spectra based on an effective model, including four anharmonic single exciton bands. Within the limitations of the model, the simulation results provide supporting evidence that there indeed is ultrafast energy transfer from Chl $c_2$ to Chl *a*. Combination of the 2D measurements and theoretical simulations allowed us to unravel excitation dynamics in this complex system. Thus, our work provides the first unambiguous determination of the light-harvesting role of Chl $c_2$ in the FCP complex.

Ultrafast energy transfer between different pigments in light-harvesting complexes implies that nature has evolved to exploit distinct properties of the available building blocks and that every pigment present has a place in a very effectively operating machinery. Exploitation of different constituents with distinct properties might help to achieve increased efficiency in artificial light-harvesting complexes.

## ■ MATERIALS AND METHODS

Sample preparation technique is described in detail in ref 28. In short, the diatom algae *C. meneghiniana* was grown under conditions of 16 h light and 8 h dark cycles. Afterward, the FCP complexes were extracted and purified by sucrose density centrifugation after the solublisation of thylakoid membranes using 20 mM dodecyl maltoside. Both FCP fractions from the gradients were harvested and pooled.

The steady state absorption spectrum of FCP and Chl $c_2$ were measured using Jasco V670 UV−vis−IR spectrometer and Jasco V500 spectrophotometer, respectively.

For pump−probe measurements, an amplified Ti:sapphire laser (Integra-C, Quantronix) was used as the light source. Pulse duration was ∼130 fs with the repetition rate of 1 kHz. The laser intensity was kept below 200 $\mu$W. Different excitation wavelengths were obtained using a tunable optical parametric amplifier (TOPAS-C, Light Conversion), while white light continuum generated in a sapphire plate was used for probing. Registration of the probe signal was done with a fiber-optic spectrometer (AvaSpec-1650F, Avantes). A mechanical stirring system was used in order to prevent localized sample degradation and thermal inhomogeneity.

For the coherent two-dimensional electronic spectroscopy, a diffractive-optics-based noncollinear four-wave mixing setup with phase-matched box geometry, heterodyne detection, and inherent phase-stabilization was used.[32,33] The light source consisted of a home-built noncollinear optical parametric amplifier pumped by an Yb:KGW amplified laser system (Pharos, Light Conversion) operating at 50 kHz repetition rate. The setup provided 680 nm (120 nm fwhm) light pulses of 15 fs duration. Additional sensitivity and noise resistance enhancement was achieved by means of double modulation lock-in detection.[33] Coherence time delay $\tau$ was scanned within a −105−132 fs interval with 1.5 fs time step employing movable fused-silica wedges. Spectrometer and dispersive delay line calibrations were performed using procedures described in ref 34. The total energy of the sample irradiation was 5 nJ/pulse, whereas the diameter of the focused beams at the sample was ∼100 $\mu$m. The specialized low-volume circulation system was used to avoid local degradation in the sample; the quartz flow cell with 0.2 mm thickness windows and 0.2 mm sample chamber ensured minimal undesirable signals from the quartz, detergent, and buffer. Optical density of the sample at 680 nm was set to about 0.3.

## ■ AUTHOR INFORMATION

### Corresponding Author

*E-mail: leonas.valkunas@ff.vu.lt.

### Notes

The authors declare no competing financial interest.

## ■ ACKNOWLEDGMENTS

The research leading to these results was funded by the European Social Fund under the Global Grant measure. Authors acknowledge support by the LASERLAB-EUROPE project (Grant Agreement No. 228334, EC's Seventh Framework Programme). V.B. acknowledges support by project "Promotion of Student Scientific Activities" (VP1-3.1-ŠMM-01-V-02-003) from the Research Council of Lithuania. Work in Lund was also supported by the Swedish Research Council and Knut and Alice Wallenberg Foundation. C.B. acknowledges funding by the Deutsche Forschungsgemeinschaft (Bu 812/4-1, 5-1). C.B., A. Gall, and B.R. acknowledge funding from the EU (HARVEST Marie Curie Research Training Network (PITN-GA-2009-238017)). B.R. acknowledges support from the European Research Council (ERC) through an Advanced Grant, Contract No. 267333.

## ■ REFERENCES

(1) Ruban, A. V. *The Photosynthetic Membrane: Molecular Mechanisms and Biophysics of Light Harvesting*; Wiley: Chichester, U.K., 2013.

(2) Falciatore, A.; Bowler, C. Revealing the Molecular Secrets of Marine Diatoms. *Annu. Rev. Plant Biol.* **2002**, *53*, 109−130.

(3) Eppard, M.; Rhiel, E. The Genes Encoding Light-Harvesting Subunits of Cyclotella cryptica (Bacillariophyceae) Constitute a Complex and Heterogeneous Family. *Mol. Gen. Genet.* **1998**, *260*, 335−345.

(4) Liu, Z.; Yan, H.; Wang, K.; Kuang, T.; Zhang, J.; Gui, L.; An, X.; Chang, W. Crystal Structure of Spinach Major Light-Harvesting Complex at 2.72Å Resolution. *Nature* **2004**, *428*, 287−292.

(5) Papagiannakis, E.; van Stokkum, I. H. M.; Fey, H.; Büchel, C.; van Grondelle, R. Spectroscopic Characterization of the Excitation Energy Transfer in the Fucoxanthin-Chlorophyll Protein of Diatoms. *Photosynth. Res.* **2005**, *86*, 241−50.

(6) Premvardhan, L.; Robert, B.; Beer, A.; Büchel, C. Pigment Organization in Fucoxanthin Chlorophyll $a/c_2$ Proteins (FCP) Based on Resonance Raman Spectroscopy and Sequence Analysis. *Biochim. Biophys. Acta* **2010**, *1797*, 1647−1656.

(7) Du, H.; Fuh, R.-C. A.; Li, J.; Corkan, L. A.; Lindsey, J. S. PhotochemCAD: A Computer-Aided Design and Research Tool in Photochemistry. *Photochem. Photobiol.* **1998**, *68*, 141−142.

(8) Gildenhoff, N.; Amarie, S.; Gundermann, K.; Beer, A.; Büchel, C.; Wachtveitl, J. Oligomerization and Pigmentation Dependent Excitation Energy Transfer in Fucoxanthin-Chlorophyll Proteins. *Biochim. Biophys. Acta* **2010**, *1797*, 543−9.
(9) Kosumi, D.; Kita, M.; Fujii, R.; Sugisaki, M.; Oka, N.; Takaesu, Y.; Taira, T.; Iha, M.; Hashimoto, H. Excitation Energy-Transfer Dynamics of Brown Algal Photosynthetic Antennas. *J. Phys. Chem. Lett.* **2012**, *3*, 2659−2664.
(10) Cho, M.; Vaswani, H. M.; Brixner, T.; Stenger, J.; Fleming, G. R. Exciton Analysis in 2D Electronic Spectroscopy. *J. Phys. Chem. B* **2005**, *109*, 10542−10556.
(11) Zigmantas, D.; Read, E. L.; Mančal, T.; Brixner, T.; Gardiner, A. T.; Cogdell, R. J.; Fleming, G. R. Two-Dimensional Electronic Spectroscopy of the B800-B820 Light-Harvesting Complex. *Proc. Natl. Acad. Sci. U.S.A.* **2006**, *103*, 12672−12677.
(12) Myers, J. A.; Lewis, K. L. M.; Fuller, F. D.; Tekavec, P. F.; Yocum, C. F.; Ogilvie, J. P. Two-Dimensional Electronic Spectroscopy of the D1−D2-cyt B559 Photosystem II Reaction Center Complex. *J. Phys. Chem. Lett.* **2010**, *1*, 2774−2780.
(13) Bixner, O.; Lukeš, V.; Mančal, T.; Hauer, J.; Milota, F.; Fischer, M.; Pugliesi, I.; Bradler, M.; Schmid, W.; Riedle, E.; et al. Ultrafast Photo-Induced Charge Transfer Unveiled by Two-Dimensional Electronic Spectroscopy. *J. Chem. Phys.* **2012**, *136*, 204503.
(14) Dostál, J.; Mančal, T.; Augulis, R.; Vácha, F.; Pšenčik, J.; Zigmantas, D. Two-Dimensional Electronic Spectroscopy Reveals Ultrafast Energy Diffusion in Chlorosomes. *J. Am. Chem. Soc.* **2012**, *134*, 11611−11617.
(15) Gelzinis, A.; Valkunas, L.; Fuller, F. D.; Ogilvie, J. P.; Mukamel, S.; Abramavicius, D. Tight-Binding Model of the Photosystem II Reaction Center: Application to Two-Dimensional Electronic Spectroscopy. *New J. Phys.* **2013**, *15*, 075013.
(16) Jonas, D. M. Two-Dimensional Femtosecond Spectroscopy. *Annu. Rev. Phys. Chem.* **2003**, *54*, 425−63.
(17) Du, J.; Teramoto, T.; Nakata, K.; Tokunaga, E.; Kobayashi, T. Real-Time Vibrational Dynamics in Chlorophyll a Studied with a Few-Cycle Pulse Laser. *Biophys. J.* **2011**, *101*, 995−1003.
(18) Abramavicius, D. Exciton-Exciton Scattering in a One-Dimensional J Aggregate. *Europhys. Lett.* **2013**, *101*, 57007.
(19) Butkus, V.; Gelzinis, A.; Valkunas, L. Quantum Coherence and Disorder-Specific Effects in Simulations of 2D Optical Spectra of One-Dimensional J-Aggregates. *J. Phys. Chem. A* **2011**, *115*, 3876−3885.
(20) Balevičius, V., Jr.; Gelzinis, A.; Abramavicius, D.; Mančal, T.; Valkunas, L. Excitation Dynamics and Relaxation in a Molecular Heterodimer. *Chem. Phys.* **2012**, *404*, 94−102.
(21) Balevičius, V., Jr.; Gelzinis, A.; Abramavicius, D.; Valkunas, L. Excitation Energy Transfer and Quenching in a Heterodimer: Applications to the Carotenoid−Phthalocyanine Dyads. *J. Phys. Chem. B* **2013**, *117*, 11031−11041.
(22) Milota, F.; Sperling, J.; Nemeth, A.; Abramavicius, D.; Mukamel, S.; Kauffmann, H. F. Excitonic Couplings and Interband Energy Transfer in a Double-Wall Molecular Aggregate Imaged by Coherent Two-Dimensional Electronic Spectroscopy. *J. Chem. Phys.* **2009**, *131*, 054510.
(23) May, V.; Kühn, O. *Charge and Energy Transfer in Molecular Systems*, 3rd ed.; Wiley-VCH: Weinheim, Germany, 2011.
(24) Valkunas, L.; Abramavicius, D.; Mančal, T. *Molecular Excitation Dynamics and Relaxation*; Wiley-VCH: Berlin, 2013.
(25) Mukamel, S. *Principles of Nonlinear Optical Spectroscopy*; Oxford University Press: New York, 1995.
(26) Abramavicius, D.; Palmieri, B.; Voronine, D. V.; Šanda, F.; Mukamel, S. Coherent Multidimensional Optical Spectroscopy of Excitons in Molecular Aggregates; Quasiparticle versus Supermolecule Perspectives. *Chem. Rev.* **2009**, *109*, 2350−2408.
(27) Metropolis, N.; Rosenbluth, A. W.; Rosenbluth, M. N.; Teller, A. H.; Teller, E. Equation of State Calculations by Fast Computing Machines. *J. Chem. Phys.* **1953**, *21*, 1087−1092.
(28) Büchel, C. Fucoxanthin-Chlorophyll Proteins in Diatoms: 18 and 19 kDa Subunits Assemble into Different Oligomeric States. *Biochemistry* **2003**, *42*, 13027−34.
(29) Polívka, T.; van Stokkum, I. H. M.; Zigmantas, D.; van Grondelle, R.; Sundström, V.; Hiller, R. G. Energy Transfer in the Major Intrinsic Light-Harvesting Complex from *Amphidinium carterae*. *Biochemistry* **2006**, *45*, 8516−8526.
(30) Blankenship, R. E. *Molecular Mechanisms of Photosynthesis*; Wiley-Blackwell: Oxford, U.K., 2002.
(31) Ratsep, M.; Linnanto, J.; Freiberg, A. Mirror Symmetry and Vibrational Structure in Optical Spectra of Chlorophyll a. *J. Chem. Phys.* **2009**, *130*, 194501.
(32) Brixner, T.; Stiopkin, I. V.; Fleming, G. R. Tunable Two-Dimensional Femtosecond Spectroscopy. *Opt. Lett.* **2004**, *29*, 884−886.
(33) Augulis, R.; Zigmantas, D. Two-Dimensional Electronic Spectroscopy with Double Modulation Lock-in Detection: Enhancement of Sensitivity and Noise Resistance. *Opt. Express* **2011**, *19*, 13126−33.
(34) Augulis, R.; Zigmantas, D. Detector and Dispersive Delay Calibration Issues in Broadband 2D Electronic Spectroscopy. *J. Opt. Soc. Am. B* **2013**, *30*, 1770−1774.